International Journal of Antimicrobial Agents 64 (2024) 107389

Contents lists available at ScienceDirect

International Journal of Antimicrobial Agents

journal homepage: www.elsevier.com/locate/ijantimicag

PK/PD modelling and simulation of longitudinal meropenem *in vivo* effects against *Escherichia coli* and *Klebsiella pneumoniae* strains with high MICs

Raphaël Saporta[a], Elisabet I. Nielsen[a], Jon U. Hansen[b], Edgars Liepinsh[c], Iris K. Minichmayr[a,d], Lena E. Friberg[a,*]

[a] *Department of Pharmacy, Uppsala University, Uppsala, Sweden*
[b] *Bacteria, Parasites & Fungi, Statens Serum Institut, Copenhagen, Denmark*
[c] *Latvian Institute of Organic Synthesis, Riga, Latvia*
[d] *Department of Clinical Pharmacology, Medical University of Vienna, Vienna, Austria*

ARTICLE INFO

Article history:
Received 4 July 2024
Accepted 11 November 2024

Editor: Dr MH Scheetz

Keywords:
PKPD
Meropenem
Carbapenem resistance
Pharmacometrics
Mouse thigh infection model

ABSTRACT

Background: Carbapenem-resistant bacteria pose a threat to public health. Characterising the pharmacokinetics-pharmacodynamics (PKPD) of meropenem longitudinally *in vivo* against resistant bacteria could provide valuable information for development and translation of carbapenem-based therapies.
Objectives: To assess the time course of meropenem effects *in vivo* against strains with high MIC to predict PK/PD indices and expected efficacy in patients using a modelling approach.
Methods: A PKPD model was built on longitudinal bacterial count data to describe meropenem effects against six *Escherichia coli* and *Klebsiella pneumoniae* strains (MIC values 32–128 mg/L) in a 24 h mouse thigh infection model. The model was used to derive PK/PD indices from simulated studies in mice and to predict the efficacy of different infusion durations with high-dose meropenem (2 g q8 h/q12 h for normal/reduced kidney function) in patients.
Results: Data from 592 mice were available for model development. The estimated meropenem concentration-dependent killing rate was not associated with differences in MIC. The fraction of time that unbound concentrations exceeded EC_{50} ($fT_{>EC50}$, EC_{50} = 1.01 mg/L) showed higher correlations than $fT_{>MIC}$. For all investigated strains, bacteriostasis at 24 h was predicted for prolonged infusions of high-dose meropenem monotherapy in >90% of patients.
Conclusions: The developed PKPD model successfully described bacterial growth and meropenem killing over time in the thigh infection model. For the investigated strains, the MIC, determined *in vitro*, or MIC-based PK/PD indices, did not predict *in vivo* response. Simulations suggested prolonged infusions of high-dose meropenem to be efficacious in patients infected by the studied strains.

© 2024 The Author(s). Published by Elsevier Ltd.
This is an open access article under the CC BY license (http://creativecommons.org/licenses/by/4.0/)

1. Introduction

Although promising antibacterial candidates are in the pipeline [1], the emergence of antimicrobial resistance (AMR)-associated infections highlights a need to optimize the use of currently available antibiotics. A previous study estimated 1.27 million deaths attributable to AMR infections on a global level in 2019 [2], with predictions suggesting that this number could increase up to 10 million a year by 2050 [3]. Meropenem-resistant bacteria are associated with clinically relevant infections. In the WHO's priority list for research and development of new antibiotics for AMR bacteria, the three bacteria types listed as critical priority pathogens are all carbapenem-resistant [4] (*Acinetobacter baumannii*, carbapenem-resistant; *Pseudomonas aeruginosa*, carbapenem-resistant; Enterobacteriaceae, carbapenem-resistant, third-generation cephalosporin-resistant). The use of high doses (e.g., 2g q8 h) and/or longer infusion durations (such as continuous infusions) of meropenem have been discussed as potential treatment options for meropenem-resistant bacteria [5–9].

Pharmacokinetic-pharmacodynamic (PKPD) studies are important to support the development of new antibiotics, as well as of dosing recommendations for available antibiotics [10]. The min-

* Corresponding author. Department of Pharmacy, Uppsala University, Box 580, 751 23, Uppsala, Sweden.
E-mail address: lena.friberg@uu.se (L.E. Friberg).

https://doi.org/10.1016/j.ijantimicag.2024.107389
0924-8579/© 2024 The Author(s). Published by Elsevier Ltd. This is an open access article under the CC BY license (http://creativecommons.org/licenses/by/4.0/)

imum inhibitory concentration (MIC) is commonly used as a PD marker in antibiotic PKPD analyses. This measure, however, does not solely represent efficacy, as strain characteristics such as growth rate may also impact the outcome of the assay. Additionally, MIC measurements provide no information about the time course of antibiotic effects given their determination at a single time point, and they do not consider virulence *in vivo*. Furthermore, the MIC is subject to both biological and assay variation [11].

To inform dose selection, PKPD studies are typically performed using neutropenic mouse infection models, in which total daily doses are split into several doses administered at different dosing intervals, with the bacterial count measured 24 h after start of treatment [12]. The MIC of the studied strain is linked to antibiotic exposure in three main PK/PD indices: area under the curve of the unbound concentration-time profile to MIC ratio (*f*AUC/MIC), maximum unbound concentration to MIC ratio (fC_{max}/MIC), and fraction of time that the unbound concentrations exceed a target concentration TC ($fT_{>TC}$, with MIC typically used as TC). To determine the index most closely related to the antibiotic response, the correlation of the response observed in the dose fractionation studies, the bacterial burden in colony-forming units (CFU), with each PK/PD index is investigated.

The PK/PD index approach is notably limited by its reliance on the MIC as an antibiotic potency marker, the evaluation of efficacy at only one time point, and the ignorance of the shape of the concentration-time profile [13,14]. PKPD modelling is a method that allows analysis of longitudinal data, i.e., to describe the time course of bacterial growth and antibiotic killing effects as represented by the change in bacterial count over time [15,16]. Given that bacterial counts are usually not determined at several time points *in vivo*, most of the published PKPD models for antibiotics are based on *in vitro* time-kill experiments rather than *in vivo* data [16].

Previous studies [17,18] have explored the ability of PKPD models for meropenem to predict PK/PD indices based on *in vitro* data. Published PKPD models for meropenem built on *in vivo* data [19,20] were based on one strain of low MIC value (*Pseudomonas aeruginosa* of MIC = 1 or 0.5 mg/L, EUCAST resistance breakpoint of 8 mg/L [21]), with a limited number of evaluated doses (1 or 4 evaluated dose groups), dosing intervals (single dose or q4 h) and time points (every 2 h over 12 h, or at start of treatment and 24 h).

This study explored the effects of meropenem monotherapy against meropenem-resistant *Escherichia coli* and *Klebsiella pneumoniae* strains across a range of doses, dosing intervals and time points using longitudinal meropenem *in vivo* mouse thigh infection data. A PKPD model was built to describe the time course of the antibiotic effect. The model was used to predict PK/PD indices of meropenem in mice against resistant bacterial strains, as well as PK/PD indices and the efficacy of high-dose meropenem in different simulated patient populations.

2. Material and methods

2.1. Mouse thigh infection model

PK and efficacy studies were performed at Statens Serum Institute (Copenhagen, Denmark) and were ethically reviewed and approved by local and national ethical committees and adhered to the national animal protection laws based on the European Directive 2010/63/EEC and Danish license No. 2016-15-0201-01049. Female BomTac:NMRI mice (Taconic Denmark) were rendered neutropenic by intraperitoneal injections of cyclophosphamide (Sendoxan, Baxter) at 4 and 1 days (approximately 200 and 100 mg/kg) prior to infection. On day 0, mice were infected by an intramuscular injection of a bacterial suspension in the left thigh to achieve the target inoculum size. MIC values were determined in triplicate by broth microdilution according to CLSI guidelines [22].

2.1.1. Pharmacokinetic studies

Mice ($n = 30$) were injected with approximately 5×10^5 *E. coli* IR57 bacteria/thigh. A single dose of 30 or 90 mg/kg of meropenem was administered subcutaneously 18 h after inoculation. Plasma samples were collected at 5, 10, 15, 30, 60 and/or 120 minutes after administration, with each mouse being sampled two to three times. Meropenem concentrations in mouse blood plasma were measured by liquid chromatography-tandem mass spectrometry (LC/MS/MS) in positive electrospray ionization (ESI+) in multi-reaction monitoring (MRM) mode, with a lower limit of quantification of 0.24 mg/L.

2.1.2. In vivo *efficacy studies*

The design of the efficacy studies was generated for a drug development program. Mice ($n = 592$) were infected with an inoculum of 5×10^5 to 6.3×10^6 bacteria/thigh. Seven isolates were evaluated (Table S1): six β-lactamase producing resistant strains (two *K. pneumoniae* and four *E. coli* strains) with meropenem MIC values 32–128 mg/L and one meropenem-susceptible *E. coli* strain, with meropenem MIC $\leq$ 0.03 mg/L. Treatment was initiated 1- or 2-h post-infection. Mice received subcutaneous meropenem doses ranging from 1 to 512 mg/kg as single administration or ranging from every 1 h to every 8 h as repeated administration. Studies also included growth control groups without meropenem administration. Mice were euthanised at the study endpoint that occurred up to 24 h after start of treatment (Table S2). Thighs were excised aseptically, homogenised, diluted and plated on agar plates. After incubation of the plates for 18 h to 22 h in ambient air at 35°C, CFU were counted.

2.2. PK modelling

One and two-compartment models with an additional depot compartment to account for absorption following subcutaneous drug administration were investigated to describe meropenem concentrations in mouse plasma. Both linear and Michaelis–Menten models were explored to describe meropenem elimination.

2.3. PKPD modelling

A PKPD model was developed using CFU count data. The base model structure assumed two bacterial population compartments: growing and drug-susceptible bacteria (S) and dormant (or resting), non-growing, non-susceptible bacteria (D) [23]. The injected inoculum was used as the initial bacterial load, and all bacteria were assumed to be in the S compartment at inoculation time. In absence of antibiotic, the bacterial system was described using Eqs. 1 and 2:

$$\frac{dS}{dt} = k_{growth} \cdot S - k_{death} \cdot S - k_{SD} \cdot S \quad (1)$$

$$\frac{dD}{dt} = k_{SD} \cdot S - k_{death} \cdot D \quad (2)$$

where k_{growth} is the bacterial growth rate constant, k_{death} describes the bacterial natural death rate constant and k_{SD} is the transfer rate constant from S to D, given by $k_{SD} = (S+D) \cdot (k_{growth} - k_{death})/B_{max}$, with B_{max} describing the maximum bacterial count in the system.

First, growth control data were analysed to estimate the bacterial parameters k_{growth}, k_{death} and B_{max}. A delay in bacterial growth

was also evaluated [24], as described by Eq. 3:

$$k_{growth}\ (T) = k_{growth_max} \cdot \frac{T^{\beta}}{T_{delay}^{\beta} + T^{\beta}} \quad (3)$$

where $k_{growth,max}$ is the post-delay growth rate, T the time since inoculation, T_{delay} the typical delay duration and β the factor describing the steepness of growth rate increase.

The developed PK model was used to predict meropenem concentrations in the efficacy studies. Parameters estimated in the growth control model were fixed, and all other data were analysed simultaneously to estimate the drug effect model. The concentration driving the drug effect C_{eff} was either considered to be the unbound concentration in the central PK compartment, or the unbound concentration in an effect compartment accounting for a delay in drug effect with a first-order rate constant k_{eff}. The unbound fraction was set to 0.81 [19]. The drug effect was implemented as a bacterial killing rate with linear or power functions (Eq. 4), or an E_{max} or sigmoid E_{max} function (Eq. 5):

$$k_{drug} = C_{eff}^{\alpha} \cdot \text{Slope} \quad (4)$$

$$k_{drug} = \frac{E_{max} \cdot C_{eff}^{Hill}}{EC_{50}^{Hill} + C_{eff}^{Hill}} \quad (5)$$

where Slope is the slope parameter, α is the power parameter ($\alpha = 1$ for linear function, $\alpha \neq 1$ for power function), E_{max} is the maximum achievable killing rate constant, EC_{50} represents the drug concentration achieving 50% of E_{max}, and Hill indicates the parameter describing the sigmoid shape (Hill = 1 for an E_{max} model, Hill ≠ 1 for a sigmoid E_{max} model). Differences in drug effect between strains were explored by using the MIC to scale the drug effect parameters.

2.4. Simulations

The developed PKPD model was used to perform simulations in a mouse thigh infection model, as well as for predictions in humans. As the original study was not designed for PK/PD index computation, PK/PD indices were computed from the simulated studies to evaluate the ability of PK/PD indices to describe the response to meropenem given the observed study design and as characterised in the PKPD model, and to further explore the relevance of the use of PK/PD indices for bacteria with high MIC.

2.4.1. Mouse PK/PD simulations and indices

The developed PKPD model was first used to simulate mouse dose fractionation studies. The initial bacterial burden was set to 10^6 CFU/thigh. Subcutaneous administration of meropenem total daily doses of 120–1560 mg/kg were simulated as a single dose, or as repeated administrations every 2, 4, or 8 h. Simulations were performed without residual variability. A sigmoid E_{max} model was evaluated for the different indices:

$$E = E_0 - \frac{PD_{max} \cdot Index^{\gamma}}{Index_{50}^{\gamma} + Index^{\gamma}} \quad (6)$$

where E is the bacterial load predicted by the model at 24 h, E_0 is the bacterial load predicted at 24 h when Index = 0, PD_{max} is the maximum drop in bacterial load from E_0 at 24 h, γ is the Hill factor for sigmoidal shape, Index is the PK/PD index value, and $Index_{50}$ is the PK/PD index value required to reach half of PD_{max}. The correlation between bacterial counts at 24 h and each PK/PD index was assessed by computing the R^2 value for the fitted sigmoid E_{max} model.

2.4.2. Human PK/PD simulations and indices

Simulations were performed to predict the efficacy and PK/PD indices of meropenem against the studied strains in humans. Two patient populations were considered, i.e., patients with normal and reduced kidney function (Table 1). A two-compartment PK model for meropenem, developed by Trang et al. [25], was used to simulate human PK profiles. High-dose intravenous administration of meropenem was simulated, covering doses recommended in the summary of product characteristics (2 g q8 h for patients with normal kidney function, 2g q12 h for patients with reduced kidney function) [26]. Different infusion durations were explored (from 0.5-h to prolonged 4-h or continuous infusions, Table 1). Unbound plasma concentrations (unbound fraction of 0.98) were used to drive the meropenem effect in the PKPD model and bacterial counts were simulated over 24 h for 1000 patients per scenario. The attainment of different efficacy targets (stasis, 1-log kill, 2-log kill) at 24 h was evaluated for all simulated patients. Additionally, the PK/PD indices were computed and correlated to the bacterial burden at 24 h with the same method as in the mouse simulations.

2.5. Data analysis and software

For the PK data, models were fit to log-transformed concentrations using an additive residual error model and the Laplacian Conditional Estimation with Interaction method in NONMEM 7.4.4 [27]. For PKPD model development, NONMEM version 7.5.0 [27], using the first-order conditional estimation with interaction method, and Perl-speaks-NONMEM (PsN) version 5.2.6 were used [28]. Data management and graphical analysis were performed using R version 4.2.1 [29]. Model selection was based on the difference in objective function value (ΔOFV), plausibility of parameter estimates, parameter uncertainty and goodness-of-fit plots [30], including visual predictive checks (VPCs) [31]. A ΔOFV of 10.83 points with one parameter difference was considered significant ($P < 0.001$). For PKPD model development, a $\log_{10}$-transform-both-side approach was used, with a $\log_{10}$-transformed additive error model. Inter-individual variability was not estimated for any parameter. Simulations were performed in R using mrgsolve version 1.0.6 [32]. Curve fitting for PK/PD indices was performed using the drc package in R [33].

3. Results

3.1. PK modelling

A one-compartment disposition model with an additional depot compartment was adequate to describe the observed plasma concentrations. The absorption rate constant k_a was initially estimated to 178 h^{-1} (RSE = 32.1%). Given that there was limited data in the absorption phase, a sensitivity analysis with k_a fixed to values reported in previous studies was performed [19,20]. The sensitivity analysis revealed that fixing k_a to lower values foremost affected C_{max} rather than the later elimination phase of the concentration-time profile, which would be important for attainment of $fT_{>MIC}$ values. In the final model, k_a was fixed to 10.2 h^{-1} according to a previous murine PK model [19]. A Michaelis–Menten elimination model did not significantly improve the model fit.

3.2. PKPD modelling

The final model structure is presented in Fig. 1. Based on growth control data, the growth rate constant k_{growth} was estimated to 0.733 h^{-1}. A delay in growth was significant (ΔOFV = 41.1), with T_{delay} estimated to 1.34 h. The sigmoidicity parameter for the delay (β) could not be estimated reliably and

Table 1
Design of the PKPD simulations for the different patient populations and infusion durations. Doses were administered intravenously. Age, weight, and eGFR for a normal kidney function correspond to the medians from the analysis population of Trang et al. [25].

Scenario	Age (years)	Weight (kg)	eGFR (ml/min/1.73 m^2)	Dose unit (mg)	Dosing interval (hours)	Infusion duration (hours)
Normal kidney function	53	75	90	2000	8	0.5, 1, 2, 4, continuous
Reduced kidney function	53	75	30	2000	12	0.5, 1, 2, 4, continuous

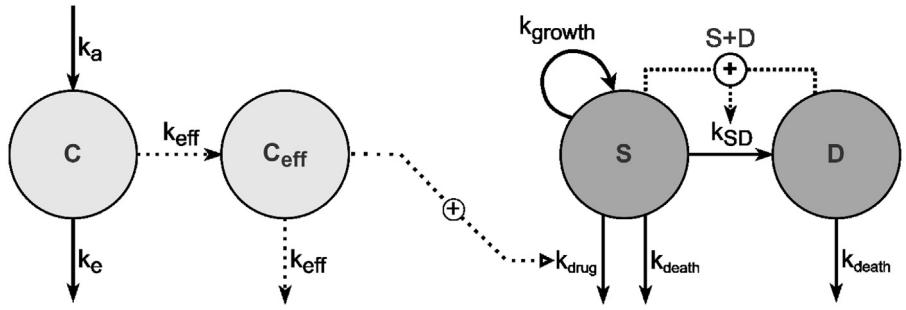

Fig. 1. Schematic representation of the PKPD model. C, meropenem plasma concentration. C_{eff}, unbound concentration of meropenem in the effect compartment. D, dormant bacteria. k_a, absorption rate constant. k_{death}, bacterial natural death rate constant. k_{drug}, meropenem effect rate constant. k_e, elimination rate constant. k_{eff}, effect compartment rate constant. k_{growth}, bacterial growth rate constant. k_{SD}, transfer to dormant state rate constant. S, susceptible bacteria.

was fixed to 5 after a sensitivity test on the other growth parameter estimates. k_{death} was fixed to 0.179 h^{-1} [23].

The addition of an effect compartment for meropenem concentrations, inducing a delay in effect after meropenem dosing with a half-life of effect delay of 0.44 h, significantly improved the model fit (ΔOFV = 47.6). The effect of meropenem was described by an E_{max} model (Hill fixed to 1), with E_{max} estimated to 0.672 h^{-1}, corresponding to a low net rate constant of change in bacterial count of -0.118 h^{-1} at E_{max} (k_{growth}-k_{death}-E_{max}) for S bacteria, corresponding to a slow decrease in bacterial counts. EC_{50} was estimated at 1.01 mg/L, a concentration 32 times below the lowest MIC among the resistant strains studied. No difference in any effect parameter between strains was identified despite 4-fold differences in MIC for the resistant strains. This E_{max} model described observations from all dose groups except the highest dose (512 mg/kg, single dose).

To account for the faster decrease in bacterial count observed in the highest dose group, an additional sigmoid E_{max} model was implemented to mimic a second type of drug effect, describing the higher killing rate at high concentrations:

$$k_{drug} = \frac{E_{max} \cdot C_{eff}}{EC_{50} + C_{eff}} + \frac{E_{max,2} \cdot C_{eff}^{Hill,2}}{EC_{50,2}^{Hill,2} + C_{eff}^{Hill,2}} \quad (7)$$

The maximum effect $E_{max,2}$ was estimated to 2.04 h^{-1} and $EC_{50,2}$ was estimated to 88.8 mg/L, a concentration within the studied MIC and concentration ranges. The sigmoidicity factor for the sigmoid E_{max} $Hill_{,2}$ was fixed to 10 following a sensitivity analysis on model fit and other effect parameter estimates. The model fit for the 512 mg/kg dose group improved with a second E_{max}, without worsening the fit for other dose groups (ΔOFV = 44.3 for two extra parameters). Scaling of the second E_{max} model parameters by MIC was not supported by the data. Precision was acceptable for all parameters (Table 2). Visual predictive checks (Fig. 2) showed good predictive performance and simulation properties for all strains, dose groups and time points.

3.3. Simulations

The delay in bacterial growth was omitted in the simulation model for mice and humans, assuming that start of treatment occurred in the log growth phase. All simulation scenarios were repeated with and without the second E_{max} model for meropenem effect. MIC was not considered when *f*AUC and *f*C_{max} were related to the 24-h response, as MIC was not used in the drug effect model and the same correlations would thus be observed for simulations with any single MIC value. $fT_{>TC}$ was computed for TC values of 32, 64 and 128 mg/L, and with TC = EC_{50} ($fT_{>EC50}$).

3.3.1. Mouse PK/PD simulations and indices

The PK/PD indices computed based on mouse simulations are presented in Fig. 3 and the R^2 values, indicating correlation between the PK/PD indices and bacterial load, are stated in Table 3. The performance of time-based indices $fT_{>TC}$ was dependent on TC selection: $fT_{>EC50}$ was the most predictive index (R^2 = 0.809 and 0.969 with/without the second E_{max} model), better than $fT_{>TC}$ indices with higher TCs, as well as compared to all other indices, for which R^2 values were low (<0.6).

3.3.2. Human PK/PD simulations and indices

The predicted meropenem effects for simulated patients are summarised in Table 4. Similar outcomes were predicted for the two populations when the dosing interval was increased from 8 h to 12 h for patients with reduced kidney function. Unbound effect compartment concentrations above EC_{50} were reached in all simulated patients, while an attainment of $EC_{50,2}$ was dependent on the infusion duration and interindividual variability (Fig. S1). Depending on the inclusion of the second E_{max} and the infusion duration, 85.6%–99.9% of patients were predicted to achieve bacterial stasis or killing at 24 h. Bacterial net growth at 24 h was predicted in a proportion of simulated patients in all scenarios, with a trend towards more growth with shorter infusion durations compared to prolonged infusions (e.g., without the second E_{max}, net growth was predicted in 0.1% of renally impaired patients with a continuous infusion, versus 14.4% with a 0.5-h infusion). However, when the second E_{max} was considered in simulations, short infusion durations were associated with higher proportions of patients reaching 2-log kill in comparison to prolonged infusions (e.g., 30.6% of renally impaired patients reached 2-log kill with a 0.5-h infusion, versus 1.3% with a continuous infusion).

The PK/PD indices for both patient populations are presented in Fig. 4, and the R^2 values are stated in Table 3. Similar results were obtained for the indices in both patient populations. When simulations were performed with a model not considering the second E_{max}, the most predictive PK/PD index was $fT_{>EC50}$ (R^2 = 0.98 in

Table 2
Parameter estimates and relative standard errors (RSE) of the final PKPD model in mice.

Parameter	Unit	Description	Estimate	RSE (%)
CL/F	L/(h•kg)	Clearance	1.72	8.3[a]
V/F	L/kg	Volume of distribution	0.994	9.5[a]
k_a	h^{-1}	Absorption rate constant	10.2	Fixed
$k_{growth,max}$	h^{-1}	Post-delay bacterial growth rate constant	0.733	4.6[b]
T_{delay}	h	Growth delay	1.35	15.2[b]
β	–	Sigmoidicity factor for growth delay	5	Fixed
k_{death}	h^{-1}	Bacterial natural death rate constant	0.179	Fixed
B_{max}	log_{10} CFU/thigh	Maximum bacterial count[c]	8.73	0.8[b]
k_{eff}	h^{-1}	Effect compartment rate constant	1.58	14.6
E_{max}	h^{-1}	Maximum meropenem effect (killing rate constant)	0.672	2.7
EC_{50}	mg/L	Concentration needed to achieve 50% of E_{max}	1.01	16.8
Hill	–	Sigmoidicity factor for the effect	1	Fixed
$E_{max,2}$	h^{-1}	Maximum meropenem second effect (killing rate constant)	2.04	29.3
$EC_{50,2}$	mg/L	Concentration needed to achieve 50% of $E_{max,2}$	88.8	10.9
$Hill_{,2}$	–	Sigmoidicity factor for the second effect	10	Fixed
RES	log_{10} CFU/thigh	Residual error (variance)	0.408	7

[a] Parameters fixed based on estimates from the PK model.
[b] Parameters fixed based on estimates from a PKPD model with growth control data only.
[c] The rate k_{SD} is dependent on the current bacterial load and related to B_{max} with $k_{SD} = (S+D) \cdot (k_{growth}-k_{death})/B_{max}$.

Table 3
R^2 of the curve fit for PK/PD indices, shown for simulations in mice and for human scenarios, and performed with or without inclusion of the second E_{max} function to capture meropenem effects. The highest R^2 value for each scenario is highlighted in bold.

Scenario	Second E_{max}	PK/PD index R^2					
		*f*AUC	*f*C_{max}	*f*$T_{>EC50}$	*f*$T_{>MIC(32)}$	*f*$T_{>MIC(64)}$	*f*$T_{>MIC(128)}$
Mouse	Yes	0.361	0.057	**0.809**	0.598	0.408	0.256
	No	0.152	0.044	**0.969**	0.441	0.147	0.183
Normal renal function patient	Yes	**0.862**	0.788	0.680	0.479	0.500	0.348
	No	0.977	NC	**0.981**	0.441	0.146	0.030
Reduced kidney function patient	Yes	**0.872**	0.776	0.657	0.524	0.576	0.394
	No	0.962	NC	**0.979**	0.463	0.182	0.038

NC: not computed.

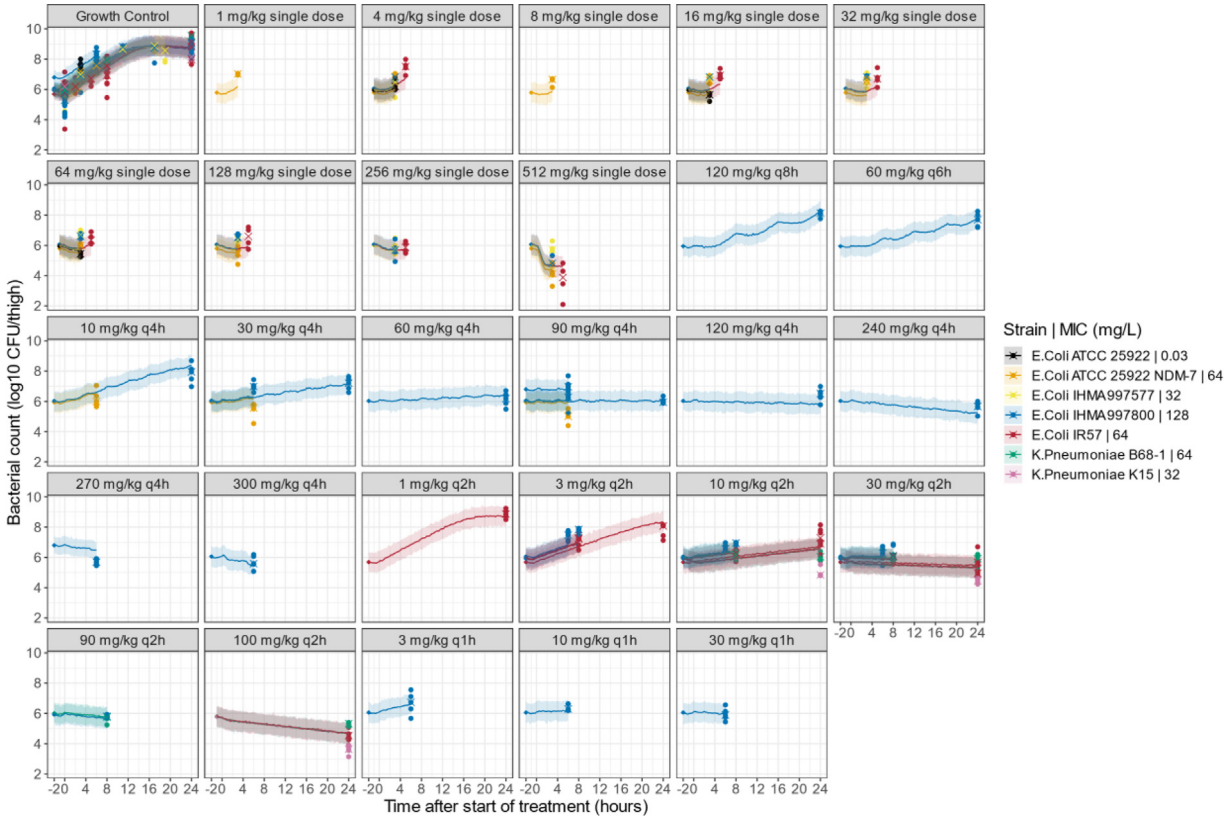

Fig. 2. Visual predictive checks of the final PKPD model. Shown are the starting inoculum (diamonds), observed (circles) and median of observed (cross) bacterial counts, with the median (lines) and 95% confidence interval around the median of the model predictions (areas) for the different meropenem dosing regimens and strains.

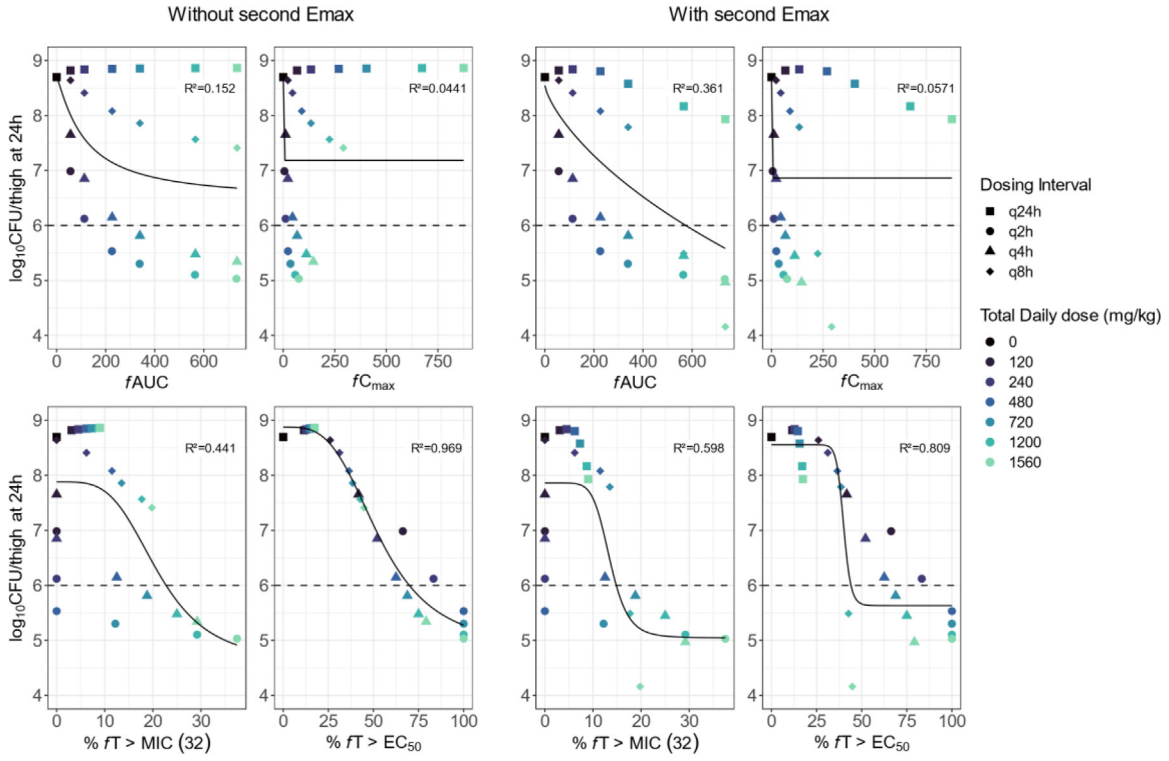

Fig. 3. Relationship between PK/PD indices and the efficacy of meropenem (bacterial load at 24 h) against resistant strains based on simulated dose-fractionation studies in the mouse thigh infection model. One mouse was simulated per dosing schedule, without variability. Shown are the predictions of bacterial count 24 h after start of treatment for each group (circles), the initial bacterial count (horizontal dashed line) and the fitted E_{max} curve (solid line). The R^2 values of the curve fits are also indicated in each panel.

Table 4
Meropenem efficacy predicted for different scenarios. The table shows the percentage of simulated patients that reached different bacterial count thresholds at 24 h after start of treatment for each simulation condition.

Infusion duration (h)	Kidney function	Second E_{max}	Growth (%)	Stasis (%)	1-log kill (%)	2-log kill (%)
0.5	Normal	Yes	8.3	47.4	17.2	27.1
		No	10	85.1	4.9	0
	Reduced	Yes	9.6	43.3	16.5	30.6
		No	14.4	82.9	2.7	0
1	Normal	Yes	7.8	51.6	15.5	25.1
		No	8.7	85.8	5.5	0
	Reduced	Yes	9.1	46.3	17.4	27.2
		No	12.4	84.6	3	0
2	Normal	Yes	3.5	61.4	18.4	16.7
		No	3.5	92.3	4.2	0
	Reduced	Yes	8.8	52.4	16.4	22.4
		No	10.4	87	2.6	0
4	Normal	Yes	0.6	78.1	13.7	7.6
		No	0.6	92.9	6.5	0
	Reduced	Yes	3	67.8	15.8	13.4
		No	3	92.6	4.4	0
C.I.	Normal	Yes	0.1	89.5	8.8	1.6
		No	0.1	94.4	5.5	0
	Reduced	Yes	0.1	94.2	4.4	1.3
		No	0.1	98.1	1.8	0

C.I.: continuous infusion; Growth: difference in bacterial count from start of treatment (dCFU) > 0 $\log_{10}$ at 24 h; Stasis: 0 ≥ dCFU > -1 $\log_{10}$ at 24 h; 1-log kill: -1 ≥ dCFU > -2 $\log_{10}$ at 24 h; 2-log kill: -2 $\log_{10}$ ≥ dCFU at 24 h.

both populations). As in the mouse simulations, $fT_{>TC}$ for higher TCs were less predictive. Using a model considering a second E_{max}, the $fT_{>EC50}$ R^2 decreased and *f*AUC appeared as the most predictive PK/PD index in both patient populations (R^2 = 0.86 and 0.87 in normal and reduced kidney functions, respectively).

4. Discussion

In this study, a PKPD model was developed to characterize the effect of meropenem over time against *E. coli* and *K. pneumoniae* strains with MICs classified to be resistant in an *in vivo* mouse thigh infection model. Differences in MIC between strains (32–128 mg/L among resistant strains) were not associated with differences in *in vivo* meropenem effects. Consequently, the TC selection impacted PK/PD index determination in mice and patients.

The developed PKPD model suggested a concentration-dependent bacterial killing over time. The estimated EC_{50} (1.01 mg/L) indicated killing at concentrations much lower than the MIC of the studied strains. A higher killing rate constant was identified at meropenem concentrations above 60 mg/L. Although

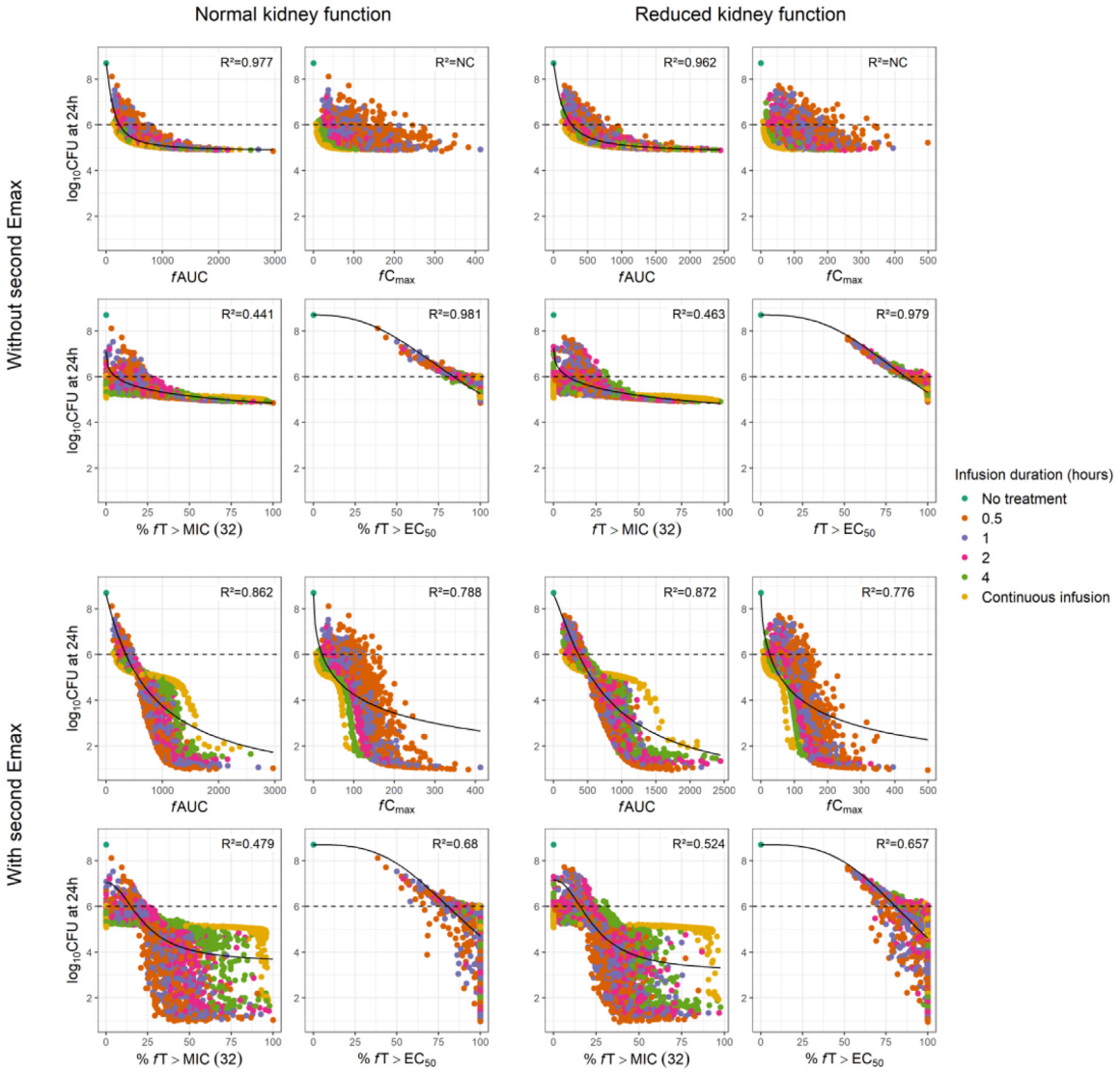

Fig. 4. Relationship between PK/PD indices and the efficacy of different infusion durations against resistant strains in a patient population with normal kidney function (administration of 2 g q8 h meropenem) and in a patient population with reduced kidney function (2 g q12 h meropenem), as predicted by the PKPD model with or without the second E_{max} function. Shown are the predictions of bacterial count at 24 h (circles), the initial bacterial count (horizontal dashed line) and the fitted E_{max} curve (solid line). The R^2 values of the curve fits are also indicated in each panel.

lower meropenem concentrations predicted stasis or 1-log kill at 24 h for certain dose groups, higher concentrations would be required to predict early killing or larger reductions in CFU at 24 h. It could be hypothesised that high meropenem concentrations allow to circumvent part of the resistance mechanisms, such as a saturation of β-lactamases, or that higher meropenem concentrations lead to higher occupancy of lower affinity penicillin-binding proteins causing an increased effect [34]. A 1- or 2-log killing at 24 h has been observed for meropenem in previous studies using mouse infection models [19,35,36]. The second E_{max} model was estimated based on all data, although the supportive information was available from the highest administered doses. Inclusion did not negatively impact the model fit for the other dose groups. Additional studies with high meropenem doses would be required to explore this relationship further and to refine the parameter estimates. Threshold concentrations leading to the higher observed killing rate could be interesting to consider when selecting an optimal dosing regimen, including rate of infusion, for infections associated with meropenem-resistant bacteria.

MIC values did not scale the meropenem effect parameters *in vivo*, suggesting similar meropenem efficacy against all studied strains despite differences in MIC. This exemplifies the limitations of using MIC as a measure of antibiotic potency *in vivo*. The MIC, an *in vitro* value, is typically the PD marker used in PK/PD indices *in vivo* [13], ignoring potential differences between experimental settings. Differences in MIC between the studied strains might be partially related to differences in virulence and growth rates *in vitro* compared to *in vivo*. The predictive ability of a PK/PD index is known to be dependent on multiple PK and PD parameters and may be influenced by the MIC [17,37]. A weak relationship between MIC and effect might also impact therapeutic drug monitoring, where targets up to 100% $fT_{>MIC}$ or 100% $fT_{>4xMIC}$ have been suggested for critically ill patients [38,39].

Simulations of mouse dose fractionation studies illustrated how MIC values not describing differences in efficacy impacted PK/PD index determination. Meropenem, like other beta-lactams, is usually associated with 'time-dependent' bactericidal killing best described by $fT_{>MIC}$ [40]. Although a similar time-dependence was

observed in the simulations, the ability to identify $fT_{>TC}$ as the best predictor of effect was dependent on the TC. As the model predicted the same effect across the studied MIC range, with killing effects observed at concentrations lower than MIC, efficacy was found for some groups with 0% $fT_{>MIC}$, in particular for higher MIC values. $fT_{>EC50}$ was identified as the best-performing PK/PD index across the bacterial strains, indicating a time-dependent trend at a concentration different from the MICs.

When the PKPD model was used to simulate high-dose meropenem administrations in two patient populations, PK/PD index determination was similarly impacted by TC selection, with $fT_{>EC50}$ performing better than $fT_{>MIC}$ for high MICs. In simulations with the model including a second E_{max} function, the most predictive index was *f*AUC. Similar predictive performance of $fT_{>MIC}$ and *f*AUC in patients, with a shift to *f*AUC as the most predictive index in populations with longer half-lives was found in a previous simulation study for meropenem [17], further highlighting the value of considering the full PK profile over a PK summary metric.

Following the recommended adjustment of meropenem dosing interval for patients with reduced renal function, similar outcomes were predicted for the two populations, with a positive outcome (stasis to 2-log kill) at 24 h for >85% of simulated patients in all scenarios. Prolonged infusions were associated with less frequent bacterial growth at 24 h (0.1% for continuous infusions). These results point to a similar direction as previous clinical studies that associated prolonged infusion of beta-lactams with a reduction of mortality [5,39,41–43]. The second E_{max} function did not impact the percentage of positive outcomes, but influenced the magnitude of the expected outcome, and resulted in predictions of 2-log kill, which was not reached in simulations not including this function. This suggests that in case of an increased effect at high concentrations, as described by the second E_{max}, the addition of a loading dose when using prolonged infusions could be valuable to achieve an early bacterial killing. Despite the fact that the *in vivo* effect was higher than expected based on the MIC, monotherapy with meropenem is expected to result in a static effect in the majority of patients (Table 4), and adding a second antibiotic might be an alternative to achieve a more rapid decline in bacterial counts, which may be of importance in a critically ill patient population. High-dose meropenem might still be a beneficial addition to therapy in cases of multi-drug resistant bacteria with limited treatment options.

The efficacy data used in this study were initially not designed for a traditional PK/PD index analysis of meropenem. This was associated with multiple benefits. Firstly, observations of bacterial count were available at multiple time points and thus allowed to characterize the time course of meropenem effect, whereas bacterial counts are commonly only observed at 24 h in standard dose fractionation study designs [12]. Secondly, a wide range of doses and dosing intervals were explored, allowing for a better description of the concentration-effect relationship.

Nonetheless, the study also had limitations. The available data included only one meropenem-susceptible strain, which was not sufficient to identify potential differences between susceptible and resistant strains. Mechanism-dependent effect parameters could not be explored since all studied resistant strains were β-lactamase producing. For several dosing regimens, data were available only at one time point and for one strain, limiting the ability to study strain differences at these doses.

To conclude, the developed PKPD model characterised the time course of meropenem *in vivo* effects on bacterial dynamics of several meropenem-resistant strains. No differences in *in vivo* effects of meropenem between strains were identified despite differences in *in vitro* MICs. Simulations notably illustrated an impact of TC on $fT_{>TC}$ performance which could influence PK/PD index determination. Simulation of outcomes in patients suggested a potential efficacy of high-dose meropenem and prolonged infusions against the studied strains.

Declarations

Funding: This project has received funding from the European Union's Horizon 2020 research and innovation program under the Marie Skłodowska–Curie grant agreement No. 861323, and the Swedish Research Council 2022-00657. The *in-vivo* research leading to these results was conducted in the ND4BB European Gram-Negative Antibacterial Engine (ENABLE) Consortium (www.nd4bb-enable.eu) and has received funding from the Innovative Medicines Initiative Joint Undertaking (www.imi.europa.eu) under grant agreement n°115583, resources of which are composed of financial contribution from the European Union's Seventh Framework Programme (FP7/2007-2013) and The European Federation of Pharmaceutical Industries and Associations (EFPIA) companies in-kind contribution.

Declaration of competing interests: None.

Ethical approval: Animal studies were ethically reviewed and approved by local and national ethical committees and adhered to the national animal protection laws based on the European Directive 2010/63/EEC and Danish license No. 2016-15-0201-01049.

Sequence information: Not applicable.

Supplementary materials

Supplementary material associated with this article can be found, in the online version, at doi:10.1016/j.ijantimicag.2024.107389.

References

[1] Butler MS, Gigante V, Sati H, Paulin S, Al-Sulaiman L, Rex JH, et al. Analysis of the clinical pipeline of treatments for drug-resistant bacterial infections: despite progress, more action is needed. Antimicrob Agents Chemother 2022;66:e01991 -21. doi:10.1128/aac.01991-21.

[2] Murray CJL, Ikuta KS, Sharara F, Swetschinski L, Aguilar GR, Gray A, et al. Global burden of bacterial antimicrobial resistance in 2019: a systematic analysis. Lancet 2022;399:629–55. doi:10.1016/S0140-6736(21)02724-0.

[3] IACG on Antimicrobial Resistance. No time to wait: securing the future from drug-resistant infections. Report to the Secretary-General of the United Nations 2019. https://www.who.int/publications-detail-redirect/no-time-to-wait-securing-the-future-from-drug-resistant-infections. (accessed 11.08.23)

[4] Tacconelli E, Carrara E, Savoldi A, Harbarth S, Mendelson M, Monnet DL, et al. Discovery, research, and development of new antibiotics: the WHO priority list of antibiotic-resistant bacteria and tuberculosis. Lancet Infect Dis 2018;18:318–27. doi:10.1016/S1473-3099(17)30753-3.

[5] Dulhunty JM, Brett SJ, De Waele JJ, Rajbhandari D, Billot L, Cotta MO, et al. Continuous vs intermittent β-lactam antibiotic infusions in critically ill patients with sepsis: the BLING III randomized clinical trial. JAMA 2024;332(8):629–37. doi:10.1001/jama.2024.9779.

[6] Song X, Wu Y, Cao L, Yao D, Long M. Is meropenem as a monotherapy truly incompetent for meropenem-nonsusceptible bacterial strains? A pharmacokinetic/pharmacodynamic modeling with Monte Carlo simulation. Front Microbiol 2019;10:2777. doi:10.3389/fmicb.2019.02777.

[7] Jaruratanasirikul S, Thengyai S, Wongpoowarak W, Wattanavijitkul T, Tangkitwanitjaroen K, Sukarnjanaset W, et al. Population pharmacokinetics and Monte Carlo dosing simulations of meropenem during the early phase of severe sepsis and septic shock in critically ill patients in intensive care units. Antimicrob Agents Chemother 2015;59:2995–3001. doi:10.1128/aac.04166-14.

[8] Oshima K, Nakamura S, Iwanaga N, Takemoto K, Miyazaki T, Yanagihara K, et al. Efficacy of high-dose meropenem (six grams per day) in treatment of experimental murine pneumonia induced by meropenem-resistant *Pseudomonas aeruginosa*. Antimicrob Agents Chemother 2017;61:e02056 -16. doi:10.1128/AAC.02056-16.

[9] Minichmayr IK, Kappetein S, Brill MJE, Friberg LE. Model-informed translation of in vitro effects of short-, prolonged- and continuous-infusion meropenem against pseudomonas aeruginosa to clinical settings. Antibiotics 2022;11:1036. doi:10.3390/antibiotics11081036.

[10] EMA Use of pharmacokinetics and pharmacodynamics in the development antibacterial medicinal products—scientific guideline. European Medicines Agency; 2018 https://www.ema.europa.eu/en/use-pharmacokinetics-pharmacodynamics-development-antibacterial-medicinal-products-scientific (accessed 18.07.23).
[11] Mouton JW, Meletiadis J, Voss A, Turnidge J. Variation of MIC measurements: the contribution of strain and laboratory variability to measurement precision. J Antimicrob Chemother 2018;73:2374–9. doi:10.1093/jac/dky232.
[12] Bulitta JB, Hope WW, Eakin AE, Guina T, Tam VH, Louie A, et al. Generating robust and informative nonclinical *in vitro* and *in vivo* bacterial infection model efficacy data to support translation to humans. Antimicrob Agents Chemother 2019;63:e02307–18. doi:10.1128/AAC.02307-18.
[13] Landersdorfer CB, Nation RL. Limitations of antibiotic MIC-based PK-PD metrics: looking back to move forward. Front Pharmacol 2021;12:770518. doi:10.3389/fphar.2021.770518.
[14] Friberg LE. Pivotal role of translation in anti-infective development. Clin Pharmacol Ther 2021;109:856–66. doi:10.1002/cpt.2182.
[15] Nielsen EI, Friberg LE. Pharmacokinetic-pharmacodynamic modeling of antibacterial drugs. Pharmacol Rev 2013;65:1053–90. doi:10.1124/pr.111.005769.
[16] Minichmayr IK, Aranzana-Climent V, Friberg LE. Pharmacokinetic/pharmacodynamic models for time courses of antibiotic effects. Int J Antimicrob Agents 2022;60:106616. doi:10.1016/j.ijantimicag.2022.106616.
[17] Kristoffersson AN, David-Pierson P, Parrott NJ, Kuhlmann O, Lave T, Friberg LE, et al. Simulation-based evaluation of PK/PD indices for meropenem across patient groups and experimental designs. Pharm Res 2016;33:1115–25. doi:10.1007/s11095-016-1856-x.
[18] Wicha S, Huisinga W, Kloft C. Translational pharmacometric evaluation of typical antibiotic broad-spectrum combination therapies against *Staphylococcus aureus* exploiting in vitro information. CPT Pharmacometr Syst Pharmacol 2017;6:512–22. doi:10.1002/psp4.12197.
[19] Katsube T, Yamano Y, Yano Y. Pharmacokinetic-pharmacodynamic modeling and simulation for in vivo bactericidal effect in murine infection model. J Pharm Sci 2008;97:1606–14. doi:10.1002/jps.21062.
[20] Louie A, Liu W, VanGuilder M, Neely MN, Schumitzky A, Jelliffe R, et al. Combination treatment with meropenem plus levofloxacin is synergistic against *Pseudomonas aeruginosa* infection in a murine model of pneumonia. J Infect Dis 2015;211:1326–33. doi:10.1093/infdis/jiu603.
[21] The European Committee on Antimicrobial Suseptibility Testing. Breakpoint tables for interpretation of MICs and zone diameters, version 14.0 2024. https://www.eucast.org/clinical_breakpoints (accessed 12.01.24).
[22] Clinical and Laboratory Standards Institute Performance standards for dilution antimicrobial susceptibility tests for bacteria that grow aerobically. 11th ed. Wayne, PA: CLSI Standard M07. Clinical and Laboratory Standards Institute; 2018.
[23] Nielsen EI, Viberg A, Löwdin E, Cars O, Karlsson MO, Sandström M. Semimechanistic pharmacokinetic/pharmacodynamic model for assessment of activity of antibacterial agents from time-kill curve experiments. Antimicrob Agents Chemother 2007;51:128–36. doi:10.1128/AAC.00604-06.
[24] Sou T, Hansen J, Liepinsh E, Backlund M, Ercan O, Grinberga S, et al. Model-informed drug development for antimicrobials: translational PK and PK/PD modeling to predict an efficacious human dose for apramycin. Clin Pharmacol Therap 2021;109:1063–73. doi:10.1002/cpt.2104.
[25] Trang M, Griffith DC, Bhavnani SM, Loutit JS, Dudley MN, Ambrose PG, et al. Population pharmacokinetics of meropenem and vaborbactam based on data from noninfected subjects and infected patients. Antimicrob Agents Chemother 2021;65:e0260620. doi:10.1128/AAC.02606-20.
[26] EMA Meronem article 30 referral. European Medicines Agency; 2009 https://www.ema.europa.eu/documents/referral/meronem-article-30-referral-annex-i-ii-iii_en.pdf (accessed 11.08.23).
[27] Beal S, Sheiner L, Boeckmann A, Bauer R. NONMEM users guides. (1989–2020). ICON plc, Gaithersburg, MD
[28] Keizer R, Karlsson M, Hooker A. Modeling and simulation workbench for NONMEM: tutorial on Pirana, PsN, and Xpose. CPT 2013;2:50. doi:10.1038/psp.2013.24.
[29] R Core Team R: a language and environment for statistical computing. Vienna, Austria: R Foundation for Statistical Computing; 2022.
[30] Nguyen THT, Mouksassi M-S, Holford N, Al-Huniti N, Freedman I, Hooker AC, et al. Model evaluation of continuous data pharmacometric models: metrics and graphics. CPT 2017;6:87–109. doi:10.1002/psp4.12161.
[31] Karlsson M, Holford N. A tutorial on visual predictive checks. Marseille: Population Approach Group Europe; 2008. p. 17.
[32] Baron K. mrgsolve: simulate from ODE-based models. 2023. https://mrgsolve.org/docs/. (accessed 18.07.23)
[33] Ritz C, Baty F, Streibig JC, Gerhard D. Dose-response analysis using R. PLoS One 2015;10:e0146021. doi:10.1371/journal.pone.0146021.
[34] Sutaria DS, Moya B, Green KB, Kim TH, Tao X, Jiao Y, et al. First penicillin-binding protein occupancy patterns of β-lactams and β-lactamase inhibitors in *Klebsiella pneumoniae*. Antimicrob Agents Chemother 2018;62:e00282 -18. doi:10.1128/AAC.00282-18.
[35] DeRyke CA, Banevicius MA, Fan HW, Nicolau DP. Bactericidal activities of meropenem and ertapenem against extended-spectrum-beta-lactamase-producing *Escherichia coli* and *Klebsiella pneumoniae* in a neutropenic mouse thigh model. Antimicrob Agents Chemother 2007;51:1481–6. doi:10.1128/AAC.00752-06.
[36] Sugihara K, Sugihara C, Matsushita Y, Yamamura N, Uemori M, Tokumitsu A, et al. In vivo pharmacodynamic activity of tomopenem (formerly CS-023) against *Pseudomonas aeruginosa* and methicillin-resistant *Staphylococcus aureus* in a Murine Thigh Infection Model. Antimicrob Agents Chemother 2010;54:5298–302. doi:10.1128/AAC.00267-10.
[37] Kitamura Y, Yoshida K, Kusama M, Sugiyama Y. A proposal of a pharmacokinetic/pharmacodynamic (PK/PD) index map for selecting an optimal PK/PD index from conventional indices (AUC/MIC, Cmax/MIC, and TAM) for antibiotics. Drug Metab Pharmacokinet 2014;29:455–62. doi:10.2133/dmpk.DMPK-14-RG-013.
[38] Abdul-Aziz MH, Alffenaar J-WC, Bassetti M, Bracht H, Dimopoulos G, Marriott D, et al. Antimicrobial therapeutic drug monitoring in critically ill adult patients: a Position Paper#. Intensive Care Med 2020;46:1127–53. doi:10.1007/s00134-020-06050-1.
[39] Hong LT, Downes KJ, FakhriRavari A, Abdul-Mutakabbir JC, Kuti JL, Jorgensen S, et al. International consensus recommendations for the use of prolonged-infusion beta-lactam antibiotics: endorsed by the American College of Clinical Pharmacy, British Society for Antimicrobial Chemotherapy, Cystic Fibrosis Foundation, European Society of Clinical Microbiology and Infectious Diseases, Infectious Diseases Society of America, Society of Critical Care Medicine, and Society of Infectious Diseases Pharmacists. Pharmacotherapy 2023;43:740–77. doi:10.1002/phar.2842.
[40] Lodise TP, Lomaestro BM, Drusano GL. Application of antimicrobial pharmacodynamic concepts into clinical practice: focus on β-lactam antibiotics. Pharmacotherapy 2006;26:1320–32. doi:10.1592/phco.26.9.1320.
[41] Vardakas KZ, Voulgaris GL, Maliaros A, Samonis G, Falagas ME. Prolonged versus short-term intravenous infusion of antipseudomonal β-lactams for patients with sepsis: a systematic review and meta-analysis of randomised trials. Lancet Infect Dis 2018;18:108–20. doi:10.1016/S1473-3099(17)30615-1.
[42] Kondo Y, Ota K, Imura H, Hara N, Shime N. Prolonged versus intermittent β-lactam antibiotics intravenous infusion strategy in sepsis or septic shock patients: a systematic review with meta-analysis and trial sequential analysis of randomized trials. J Intensive Care 2020;8:77. doi:10.1186/s40560-020-00490-z.
[43] Aboulatta L, Sugita H, Wakabayashi H, Noma H, Sasaki T. Comparison of extended versus intermittent infusion of antipseudomonal beta-lactams for the treatment of critically ill patients with respiratory infections: a systematic review and meta-analysis. Int J Infect Dis 2020;98:41–50. doi:10.1016/j.ijid.2020.06.022.